



1 **Field Investigations of Coastal Sea Surface Temperature Drop**  
2 **after Typhoon Passages**

3 Dong-Jiing Doong <sup>[1]\*</sup> Jen-Ping Peng <sup>[2]</sup> Alexander V. Babanin <sup>[3]</sup>

4 <sup>[1]</sup> Department of Hydraulic and Ocean Engineering, National Cheng Kung University, Tainan,  
5 Taiwan

6 <sup>[2]</sup> Leibniz Institute for Baltic Sea Research Warnemuende (IOW), Rostock, Germany

7 <sup>[3]</sup> Department of Infrastructure Engineering, Melbourne School of Engineering, University of  
8 Melbourne, Australia

9 ----

10 **\*Corresponding author:**

11 Dong-Jiing Doong

12 Email: [doong@mail.ncku.edu.tw](mailto:doong@mail.ncku.edu.tw)

13 Tel: +886 6 2757575 ext 63253

14 Add: 1, University Rd., Tainan 70101, Taiwan

15 Department of Hydraulic and Ocean Engineering, National Cheng Kung University

16



1

## Abstract

2 Sea surface temperature (SST) variability affects marine ecosystems, fisheries, ocean primary  
3 productivity, and human activities and is the primary influence on typhoon intensity. SST drops  
4 of a few degrees in the open ocean after typhoon passages have been widely documented;  
5 however, few studies have focused on coastal SST variability. The purpose of this study is to  
6 determine typhoon-induced SST drops in the near-coastal area (within 1 km of the coast) and  
7 understand the possible mechanism. The results of this study were based on extensive field data  
8 analysis. Significant SST drop phenomena were observed at the Longdong buoy in northeastern  
9 Taiwan during 43 typhoons over the past 20 years (1998–2017). The mean SST drop ( $\Delta$ SST)  
10 after a typhoon passage was 6.1 °C, and the maximum drop was 12.5 °C (Typhoon Fungwong  
11 in 2008). The magnitude of SST drop was larger than most of the observations in the open ocean.  
12 The mean duration of SST drop was 24 hours, and on average, 26.1 hours were required for the  
13 SST to recover to the original temperature. The coastal SST drops at Longdong were correlated  
14 with the moving tracks of typhoons. When a typhoon passes south of Longdong, the strong and  
15 persistent longshore winds induce coastal upwelling and pump cold water up to the surface,  
16 which is the dominant cause of SST drops along the coast. In this study, it was determined that  
17 cold water mainly intruded from the Kuroshio subsurface in the Okinawa Trough, which is  
18 approximately 50 km from the observation site. The magnitude of coastal SST drops depends  
19 on the area of overlap between typhoons generating strong winds and the Kuroshio. The dataset  
20 used in this study can be accessed by <https://doi.pangaea.de/10.1594/PANGAEA.895002>.

21 Keywords: Coastal SST drop, Typhoon, Upwelling, Kuroshio, Data buoy

22

## 23 1. Introduction

24 Similar to the Earth's atmosphere, sea surface temperature (SST) changes diurnally, but the  
25 range is small. Significant SST drops ( $\Delta$ SST) after typhoon (hurricane) passages have been



1 widely known and reported in the world's oceans, including the Northwest Pacific (Sakaida et  
2 al., 1998; Tsai et al., 2008a, 2008b, 2013; Chen et al., 2003; Wada et al., 2005, 2009; Chang et  
3 al., 2008; Wu et al., 2008; Morimoto et al., 2009; Hung et al., 2010; Kuo et al., 2011; Sun et al.,  
4 2015; Subrahmanyam, 2015), Northeast Pacific (Bingham, 2007), India Ocean (Rao et al., 2004;  
5 Gopalakrishna et al., 1993), and South China Sea (Shang et al., 2008; Jiang et al., 2009; Tseng  
6 et al., 2010; Chiang et al., 2011). SST drops are larger in scale following a typhoon passage  
7 than under regular temperature variability and may affect marine ecosystems and the primary  
8 productivity of the ocean (Lin et al., 2003b; Siswanto et al., 2007). Cold water increases  
9 nutrients for marine life. Several studies (Babin et al., 2004; Hanshaw et al., 2008; Liu et al.,  
10 2009; Kawai and Wada, 2011, Cheung et al., 2013; Xu et al., 2017) have reported that  
11 chlorophyll-*a* increases when SST drops after the passages of tropical cyclones. In contrast, fish  
12 species that cannot tolerate cold may die if the water temperature drops dramatically over a  
13 short period of time. In addition, the water temperature has a major impact on human comfort  
14 and safety during swimming, surfing, and snorkeling activities.

15 Upwelling and entrainment (vertical mixing) have been identified as the main causes of sea  
16 surface water temperature cooling after a typhoon passage (Price, 1981; Rao et al., 2004;  
17 Narayan et al., 2010; Shen et al., 2011; Chen et al., 2012). The maximum SST drop caused by  
18 typhoons rarely exceeds 6 °C (Wentz et al., 2000). Price (1981) presented SST drops of 3 °C  
19 and 1 °C in US waters during Hurricane Eloise in 1975 and Hurricane Belle in 1976,  
20 respectively. He noted that the SST decrease beneath a moving hurricane was mainly caused by  
21 entrainment and that the heat changes in the air and sea play minor roles. Stronger wind stress  
22 and the associated curl surface wind trigger more substantial ocean mixing and induce the  
23 mixing of sea surface water with colder and deeper waters. Wada et al. (2009) studied the role  
24 of vertical turbulent mixing (VTM) in sea surface cooling during typhoon Rex in 1998 in the  
25 Northwestern Pacific Ocean near Japan, during which the SST dropped by nearly 3 °C. They



1 concluded that sea surface cooling was caused by shear-induced VTM during the fast-moving  
2 phase of the typhoon; in contrast, sea surface cooling was caused by Ekman pumping during  
3 the slow phase of the typhoon. Notably, unless the waters are very shallow, the wind-mixing  
4 mechanism usually occurs through the action of wind-generated waves. Such wave-induced  
5 mixing has been studied in tropical cyclone conditions (Ghantous and Babanin, 2014) and  
6 through measurements obtained during tropical cyclones (Toffoli et al., 2012), and this mixing  
7 was shown to cool the surface on a scale of a few hours of cyclone forcing. Turbulence plays  
8 an important role in the heat, momentum, and energy balances of the ocean. Huang et al. (2012)  
9 measured the upper ocean turbulence dissipation associated with wave-turbulence interactions  
10 in the South China Sea. Their results contribute to understanding the SST drop induced by wave  
11 mixing.

12 The South China Sea (SCS) is one of the largest semienclosed marginal seas subject to frequent  
13 typhoons. Chiang et al. (2011) reported that the average SST cooling in the northern SCS during  
14 typhoon passage was approximately  $4.3 \pm 2$  °C in 1958~2008. Tseng et al. (2010) and Lin et al.  
15 (2003) observed an SST drop of more than 9 °C in the northern SCS during Typhoon Kaitak in  
16 2000. They concluded that this drastic SST drop could mainly be ascribed to continual wind-  
17 forced upwelling, a preexisting, relatively shallow thermocline, local bathymetry, and a slow  
18 propagation speed of typhoons. Furthermore, Chiang et al. (2011) estimated that the upwelling  
19 contribution to SST drop is twice that of entrainment for the case of Typhoon Kaitak in 2000.  
20 A larger SST drop in the central SCS was observed by Shang et al. (2008) during Typhoon  
21 Lingling in 2001. Prior to Typhoon Lingling, the SST was approximately 27~30 °C; however,  
22 the SST was reduced by 11 °C after the typhoon passed. This extreme SST drop was mainly  
23 attributed to preexisting eddies that were driven by the northeast monsoon. Zheng et al. (2010)  
24 also considered that preexisting eddy is a favored condition for intensive cooling after typhoon  
25 passage.



1 SST drops also frequently occur in the waters off northeastern Taiwan. Kuroshio flows through  
2 this region, which is the most important current that transports warm water from the tropical  
3 ocean. The SST drop off northeastern Taiwan mainly occurs during the winter monsoon rather  
4 than the summer season (Tsai et al., 2008a; Jan et al., 2013). Bathymetry-induced upwelling,  
5 rather than entrainment mixing, is considered to be the primary cause of SST drops in this region  
6 (Tsai et al., 2008). The numerical modeling results of Tsai et al. (2008b; 2013) suggest that the  
7 Taiwan Strait outflow is blocked by northerly winds, facilitating Kuroshio intrusion and thus  
8 leading to SST drops during the first half of a typhoon passage. This mechanism is similar to  
9 that involved in the winter monsoon. In contrast, Morimoto et al. (2009) demonstrated that the  
10 northward flow of the Kuroshio is mainly because of the continuous, strong southerly winds,  
11 which accelerate the Kuroshio and force its axis shoreward, resulting in the intrusion of the  
12 Kuroshio towards the shelf and SST drops offshore. Furthermore, Wu et al. (2008) indicated  
13 that internal waves were generated after Typhoon Nari's departure in 2001 and that this was a  
14 minor cause of SST drops. SST drops that occur after typhoon passage are rapid and occur  
15 within a short period of time (Tsai et al., 2013). According to previous studies, these temperature  
16 decreases in the waters off northeastern Taiwan are approximately 4~8 °C after typhoon passage  
17 (Chang et al., 2008; Wu et al., 2008; Tsai et al., 2008a).

18 Table 1 summarizes the records of SST drops after typhoon passages reported in the literature.  
19 Most studies on drops in SST have been conducted in the open ocean. There have been  
20 comparatively few studies conducted on near-coastal waters (i.e., less than 1 kilometer from the  
21 coastline). In addition, most previous studies on SST drops have been conducted based on  
22 numerical modeling or satellite images because long-term field observations of SSTs are  
23 relatively rare in typhoon-prone areas. Thus, the purpose of this research is to study SST drops  
24 following typhoon passages in coastal areas. Unlike previous studies, this study was conducted  
25 based on an analysis of field data. Coastal SST variability substantially affects both coastal



1 environmental ecosystems and human activities, and therefore, typhoon-induced coastal SST  
2 variability requires a dedicated study.

3

## 4 **2. Study area and data**

### 5 **2.1 Study area**

6 This research was conducted on the Longdong coast in northeastern Taiwan, as shown in Figure  
7 1. The Longdong coast is characterized by its irregular coastline and rapidly changing  
8 bathymetry. The Longdong coastline is oriented northwest-southeast at approximately 160  
9 degrees from north. The average sea bottom slope at Longdong is  $\sim 1/50$ . An important North  
10 Pacific warm western boundary current, known as Kuroshio, flows along the eastern waters of  
11 Taiwan. The observed maximum flow velocity of Kuroshio varies between 0.7 and 1.4 m/s and  
12 is located at depths ranging from 20 m to 100 m (Jan et al., 2011). The distance between  
13 Taiwan's coast and the main stream of Kuroshio is varied. Morimoto et al. (2009) demonstrated  
14 that the western edge of the Kuroshio stream flows approach Taiwan during the typhoon period.  
15 In this study, the shift in Kuroshio during typhoon Haitang in 2005 is estimated and plotted in  
16 Figure 1, according to Morimoto et al. (2009).

### 17 **2.2 Data**

#### 18 **2.2.1 SST measured by moored buoys**

19 SST can be measured by satellite technology, ships, and floating or moored buoys (Matthews,  
20 2013). Satellite observations provide the spatial distribution of SST; however, moored buoys  
21 record the time series of SST. In this study, the main data are the SST recorded by a 2.5-meter  
22 disc-shaped buoy deployed in the water along the Longdong coast. The Longdong buoy was  
23 deployed by the Coastal Ocean Monitoring Center of National Cheng Kung University, as  
24 assigned by the Taiwan Central Weather Bureau (CWB) in 1998. This buoy is approximately



1 0.6 km off the Longdong coast and is situated in the water at 23 m depth. The buoy is anchored  
2 to the sea bottom. The buoy was equipped with sensors of water and air temperatures, wind,  
3 pressure and wave, as well as power unit, data transmission unit and control unit. Every hour,  
4 the buoy automatically switches on to collect the oceanographic and atmospheric data. The  
5 sampling rates for all sensors are 2 Hz. The sampling duration for wind and wave data is 10  
6 minutes to the hour and it is 1 minute to the hour for pressure and temperature data. The water  
7 temperature sensor is installed at 0.6 m below the sea surface. The procedures of sensor  
8 calibration, system integration, operation and maintenance have been qualified by ISO  
9 9001:1994 since 2000.

10 The SST is measured by a platinum resistance temperature detector (RTD) which is capable to  
11 cover the range from -10 to 70 degrees Celsius. The sensor provides  $\pm 0.1\%$  F.S. accuracy for  
12 critical temperature monitoring applications. Before integrating the temperature sensor with the  
13 buoy, the sensor is submitted to the National Meteorological Instruments Center in CWB for  
14 calibration to confirm the sensor accuracy. All new or retrieved sensors from the field were  
15 submitted for calibration. After integrating the water temperature sensor into the buoy, the  
16 temperature measurements are compared with those of another sensor to confirm the system's  
17 accuracy before sea deployment. The buoy SST data used in this study can be accessed by  
18 <https://doi.pangaea.de/10.1594/PANGAEA.895002>.

#### 19 2.2.2 Water temperature measured by tide station

20 In addition to the Longdong buoy, SST data were also collected from buoys at the Gueishandao,  
21 Suao, and Hualien and tide stations at Linshanbi, Keelung and Fulong, respectively. The  
22 locations of these stations are shown in Figure 1. The buoys at Gueishandao, Suao and Hualien  
23 are 10.0 km, 1.0 km, and 0.6 km from the coast and are situated in the water at depths of 38 m,  
24 20 m, and 21 m, respectively. All tide stations are located inside the harbors and are equipped  
25 with water temperature sensors installed at the bottoms (depth varies from 2 to 5 m) of the



1 stations. The SST data from tide stations and used in this study can be accessed by  
2 <https://doi.pangaea.de/10.1594/PANGAEA.895002>.

### 3 2.2.3 Current data

4 Current data observed by acoustic Doppler current profilers (ADCPs) deployed at Longdong  
5 and Linshanbi were also collected and used for validation. The ADCPs were bottom-mounted  
6 and up-looking and measured the current profile of the sea column. Current data from the  
7 Longdong ADCP were collected from June 2008 to June 2009 and data from four typhoons  
8 (Kalmaegi, Fungwong, Sinlaku, and Jangmi) were recorded. The Linshanbi ADCP only  
9 obtained recordings in September 2013, which included data from the passage of Typhoon  
10 Usagi. The current data used in this study can be accessed by  
11 <https://doi.pangaea.de/10.1594/PANGAEA.895002>.

### 12 2.2.4 Satellite images

13 Except for the field data, multiscale ultra-high resolution (MUR) SST satellite images  
14 (downloaded from the NOAA website:  
15 [http://coastwatch.pfeg.noaa.gov/erddap/griddap/jplMURSST.graph?analyzed\\_sst](http://coastwatch.pfeg.noaa.gov/erddap/griddap/jplMURSST.graph?analyzed_sst)) were also  
16 collected for cross analysis. In an optimal way, this dataset combines data from the advanced  
17 very high resolution radiometer, moderate imaging spectroradiometer's Terra and Aqua, and  
18 advanced microwave spectroradiometer-EOS instruments to produce 1-km global SST maps.  
19 Data have been released since 2003, and one image is produced per day. The SST images during  
20 Typhoon Jangmi in 2008 were collected in this study.

### 21 2.2.5 Spatial wind field

22 To discuss the possible mechanism of SST drop, the cross-calibrated multiplatform (CCMP)  
23 gridded surface vector winds for the East Asia area (115-130°E, 18-30°N) were collected.  
24 CCMP is one of the productions provided by the scientific research company, Remote Sensing  
25 Systems (RSS), located in California, USA. The CCMP version 2.0 dataset integrates



1 observations from satellites, moored buoys, and model results and provides a long-term and  
2 high resolution record of global ocean surface (10 m) winds (Wentz et al., 2015). The spatial  
3 and temporal resolutions of CCMP wind are 0.25 degree and 6 hours, respectively. CCMP has  
4 a wide-ranging appeal to users in educational, operational and research environments. In this  
5 study, data obtained during Typhoon Bilis in 2000, Fungwong in 2008, Morakot in 2009 and  
6 Fanapi in 2010 were downloaded from <http://www.remss.com/measurements/ccmp>.

### 7 **2.3 Data quality check**

8 Checking data quality is necessary and crucial to field data analysis. Incorrect data may yield  
9 misleading results, and inaccurate observations may have a greater negative impact than a lack  
10 of observations. In addition to the satellite image and wind field data that were downloaded  
11 from qualified websites, all field data were strictly verified. The list of field data used in this  
12 study are shown in Table 2. The field measurements are equipped with a solid data quality  
13 checking (QC) system (Doong et al., 2007), including both automatic and manual verifications  
14 of raw data and statistical data, respectively. The automatic machine verification is used to cull  
15 out the suspicious data according to the rationality, continuity, and correlation of data. The  
16 manual verification is used to double check the suspicious data according to spectrum, nearby  
17 observations and the QC engineers' knowledge and experiences. Except for QC procedures,  
18 data are correlated with nearby measurements every month, season and year to develop quality  
19 accuracy (QA) and increase confidence in the data use. Figure 2 shows one SST drop event in  
20 2013 during Typhoon Usagi as an example. The SST drops were measured by the Longdong  
21 buoy, Longdong ADCP, and Linshanbi tide station. The simultaneous observations of SST  
22 drops using different instruments proves that the phenomenon cannot be ascribed to  
23 instrumental error.

### 24 **2.4 Typhoons**

25 There were 108 typhoon datasets observed by the Longdong buoy from 1998 to 2017. Typhoons



1 are complex atmospheric phenomena and have high variabilities in intensity, moving track, and  
2 speed; therefore, not all typhoons induced SST drops. For forty-three typhoons, significant SST  
3 drops along the coast of Longdong. Table 3 shows the list of the cases. The intensity of the  
4 typhoons is categorized according to the Saffir-Simpson classification method. The maximum  
5 significant wave height of each typhoon is shown in the table. Typhoon parameters are highly  
6 time dependent. The values of typhoon intensity and maximum sustained wind shown in Table  
7 3 are the numbers obtained when the typhoons were closest to Taiwan.

### 8 **3. Data Availability**

9 The dataset used in this study was deposited in the World Data Center PANGAEA  
10 (<https://doi.pangaea.de/10.1594/PANGAEA.895002>). The contents and format of the data are  
11 included in the “readme” file provided with the data.

12

### 13 **4. Statistics on coastal SST drop**

#### 14 **4.1 SST drop determination**

15 To estimate the scale and rate of each SST drop event, the starting and ending times and  
16 temperatures of an SST drop process were determined. The background SST, which is defined  
17 as the mean SST over the seven days before the SST drop occurrence, is first obtained to  
18 determine the starting point of the event. The starting time of each SST drop event was defined  
19 based on the point at which the water temperature rapidly dropped to a value lower than the  
20 background SST. The lowest SST was the minimum water temperature value during the  
21 typhoon. The  $\Delta$ SST was the difference between the background SST and the lowest SST. The  
22 duration and further cooling rate of an SST drop event are then estimated. The cooling rate  
23 represents how rapidly a typhoon exerted effects on the ocean.

#### 24 **4.2 The significant coastal SST drop event**



1 Typhoon Fungwong occurred in 2008 and was a Category II typhoon when it was close to  
2 Taiwan. The typhoon exhibited a maximum wind speed of 43 m/s and a minimum central air  
3 pressure of 948 hpa. Fungwong occupied an area at 22°N and 136°E and traveled approximately  
4 along the latitude of 22°N at an average speed of 4.7 m s<sup>-1</sup>. The intensity of the typhoon  
5 increased to that of a medium typhoon during the second half of July 26 and subsequently  
6 changed direction to the northwest. Figure 3 shows the track of the typhoon and the time series  
7 of the SST, wind speed, wind direction, and significant wave height observed at the Longdong  
8 buoy during Fungwong. Before the typhoon approached, the background SST was 29.1 °C. The  
9 mean wind speed was lower than 10 m/s, and the wind directions were irregular. On July 28,  
10 Fungwong landed on the eastern coast of Taiwan, and the mean wind speed at Longdong rapidly  
11 increased and reached a maximum value of 21.4 m s<sup>-1</sup>. The wind direction shifted northward  
12 and continued for approximately one day. The significant wave height increased to 7.9 m on  
13 July 28 from less than 0.5 m on July 26. Approximately 7 hours later, the SST began to drop.  
14 Cold water at a temperature of 16.6 °C was observed on July 29. The total SST drop was 12.5  
15 °C within 17 hours. Then, the SST took 35 hours to recover to its background temperature level.  
16 Typhoon Fungwong in 2008 induced the maximum SST drop in Longdong.

### 17 **4.3 Statistical results**

18 To reduce the measurement uncertainty, only SST drops larger than 2 °C were considered in  
19 this study. Forty percent (43 of 108) of typhoons triggered a significant SST drop in Longdong  
20 in the past 20 years (1998-2017). Among these 43 typhoons, the mean SST drop was 6.1 °C,  
21 and the maximum drop was 12.5 °C (Typhoon Fungwong in 2008). The mean drop duration  
22 was 24 hours, and the mean recovery duration was 26.1 hours. The mean cooling rate was 0.32  
23 °C/hr; however, the maximum cooling rate reached 0.83 °C/hr, which occurred during Typhoon  
24 Bilis in 2000. Figure 4 shows the distribution of the SST drop magnitude. Typhoon passages  
25 that caused SSTs to drop by 3~4 °C occurred most frequently. Six typhoons caused coastal SSTs



1 to drop by more than 10 °C. These include Typhoon Bilis in 2000, Fungwong in 2008, Morakot  
2 in 2009, Fanapi in 2010, Matmo in 2014, and Megi in 2016. The typhoon tracks and time series  
3 of SSTs are shown in the Appendix. The intensities of Typhoon Fungwong (Category II) and  
4 Morakot (category I) were relatively weak, but these typhoons induced the largest and second-  
5 largest SST drops on the Longdong coast.

6

## 7 **5. Mechanisms of coastal SST drop**

### 8 **5.1 Typhoon dependence**

#### 9 5.1.1 Typhoon Intensity

10 The scale of the typhoon-induced SST drop depends on the typhoon's characteristics, such as  
11 the intensity measured by the maximum surface wind speed, moving speed and size. Zhu et al.  
12 (2006) quantified the influence of SST variability on typhoon intensity using a numerical model.  
13 However, this is not the case for the coastal ocean at Longdong. Of the 43 typhoons that  
14 triggered significant coastal SST drops, there were 8 categorized as category I typhoons, 7  
15 category II typhoons, 8 category III typhoons, 8 category IV typhoons, and 8 category V  
16 typhoons. Another 4 typhoons were categorized as tropical storms (TS). The uniform intensity  
17 distribution of all typhoons causing SST drops demonstrates that intensity may not be a  
18 significant factor triggering the coastal SST drop. This can also be validated according to weak  
19 typhoons (for example, Typhoon Hagibis in 2014) that triggered larger coastal SST drops than  
20 stronger typhoons (for example, category IV Typhoon Tembin in 2012). We used both the  
21 minimum central air pressure and central maximum wind speed as typhoon intensity indicators  
22 to understand their influences on SST drops. The regression results show that the determination  
23 coefficients of the typhoon intensity indicators with the SST drop scale ( $\Delta$ SST) were smaller  
24 than 0.15. Again, it was suggested that typhoon intensity is not the dominant factor that  
25 influences coastal SST drops.



### 1 5.1.2 Typhoon track and moving speed

2 We classify typhoon moving tracks into five paths, as shown in Figure 5. Tracks A, B, and C  
3 represented typhoons that traveled from southeast to northwest. Track A was north of waters  
4 off Longdong, whereas tracks B and C were south of Longdong. Typhoons on track B made  
5 landfall, whereas track C typhoons traveled along Southern Taiwan. The typhoon numbers (of  
6 a total of 43 cases) and their corresponding mean temperature decreases for each track are listed  
7 in Figure 5. Typhoons that traveled along tracks B and C occupied 70% of those typhoons that  
8 triggered SST drops, and the mean decrease in temperature for the sea surface at Longdong is  
9 greater than 6 °C (7.6 °C for track B; 6.4 °C for track C). This indicates that the mean distance  
10 between track C typhoons and Longdong is more than 500 km. Typhoons that traveled along  
11 track A were closer to the waters off Longdong, but of the typhoons that induced an SST  
12 decrease along this track, the scale of SST decrease was relatively small. Typhoons that passed  
13 along the south side of Longdong had greater induced SST drops than other typhoons. These  
14 results were consistent with those of previous studies conducted in the open ocean (Price, 1981;  
15 Wada et al., 2005; 2009), which have proposed that the SST response is larger on the right side  
16 of a typhoon.

17 Slow-moving typhoons induced larger SST drops in the open sea because they facilitate more  
18 substantial air-sea interactions (Tsai et al., 2008; Wada et al., 2009; Tseng et al., 2010; Kuo et  
19 al., 2011). This study correlated the typhoon moving speeds with the magnitude of coastal SST  
20 drops and found no correlation (coefficient of determination is 0.02).

### 21 5.1.3 Typhoon wind distribution

22 The above results show that the coastal SST drop at Longdong is correlated with the typhoon  
23 track. Therefore, it is interesting to look directly at the wind distribution during typhoons.  
24 Figure 6 shows the CCMP wind patterns for the four significant cases (Typhoon Bilis in 2000;  
25 Fungwong in 2008; Morakot in 2009; and Fanapi in 2010). Because of the output time limitation



1 for the operational model, the CCMP wind fields are not exactly at the starting time of SST  
2 drop, but the maximum values are different within 2 hours. All 4 cases show strong winds off  
3 the northeast Taiwan waters, and the wind directions are parallel with the Kuroshio direction.  
4 The coverage of the Kuroshio region with large wind speeds is a significant factor. We found  
5 that when the area of strong wind overlapping with Kuroshio is large (for example, Typhoons  
6 Fungwong and Morakot in Figure 6b and 6c), there was a very large SST drop along the  
7 Longdong coast. We suggest that the interaction between typhoon wind and Kuroshio plays an  
8 important role in triggering coastal SST drops in the northeast corner of Taiwan.

## 9 **5.2 Vertical Kuroshio intrusion**

10 Seeking the source of the cold waters is the most interesting issue in this study. Because the  
11 Longdong buoy observation site is located in near-coastal water (0.6 km from the coastline at  
12 23 m water depth), the cold waters may originate from three sources: river discharge from the  
13 land, adjacent surface water, or subsurface water.

14 The Shuangsi River is the only stream near Longdong. However, the discharge of the river is  
15 small, and the river water temperature ranges between 26 to 30 °C during the summer typhoon  
16 season, although the mean low SST in the waters off Longdong was 21.5 °C. This fact allows  
17 for rejection of the hypothesis that cold waters were supported by land.

18 We assume that the cold waters were pumping from the subsurface of Longdong. According to  
19 the simultaneous measurement of wind, we observed southerly winds during the SST drop  
20 periods (Figure 3 and Figure 6, as examples). The prevailing wind directions during these  
21 typhoons were between 164° and 189°. The Longdong coastline lies at an angle of 160°  
22 from north. Thus, typhoons created winds parallel to the Longdong coastline and induced  
23 coastal upwelling. The subsurface water is usually cooler than the surface water it replaces. To  
24 prove this assumption, the current profile data were analyzed.

25 The current profile data were measured very close to the Longdong buoy by an ADCP from



1 2008 to 2009. There were four typhoon-induced surface cooling cases observed during the  
2 ADCP measurement period: Typhoon Kalmaegi ( $\Delta\text{SST} = 5.1\text{ }^{\circ}\text{C}$ ), Typhoon Fungwong ( $\Delta\text{SST}$   
3  $= 12.5\text{ }^{\circ}\text{C}$ ), Typhoon Sinlaku ( $\Delta\text{SST} = 6.8\text{ }^{\circ}\text{C}$ ), and Typhoon Jangmi ( $\Delta\text{SST} = 8.0\text{ }^{\circ}\text{C}$ ). The  
4 current profiles obtained during Typhoon Fungwong are shown in Figure 7. In the waters off  
5 Longdong, currents flowed offshore while the alongshore winds blew during typhoons. The sea  
6 current in the area generally flows shoreward, but instead, the current flowed seaward. The data  
7 demonstrated that typhoons generate an alongshore wind and pump cold water from the  
8 subsurface of Longdong to cool the surface.

9 The mean SST drop in the waters off Longdong was estimated to be  $6.1\text{ }^{\circ}\text{C}$ ; however, the  
10 Longdong buoy is situated in water that is 23 m deep. The difference in water temperature  
11 between the sea surface and sea bottom is only approximately  $2\sim 3\text{ }^{\circ}\text{C}$ . It was assumed that the  
12 observed cold water was not from the subsurface water at the Longdong buoy location but may  
13 be transferred from offshore deep sea waters. In this study, we referred to the data of the mean  
14 water temperature profile from the Ocean Data Bank (ODB) of the Ministry of Science and  
15 Technology of Taiwan. The data have been collected by research vessels since 1985. At a deep  
16 sea location ( $122.5^{\circ}\text{E}$ ,  $25.25^{\circ}\text{N}$ ) in waters off Longdong, the temperature is  $22.9\text{ }^{\circ}\text{C}$  at a depth  
17 of 50 m,  $18.8\text{ }^{\circ}\text{C}$  at 100 m and  $14.5\text{ }^{\circ}\text{C}$  at 200 m. The mean lowest SST for those 43 events was  
18  $21.5\text{ }^{\circ}\text{C}$  and was  $16.1\text{ }^{\circ}\text{C}$  for the extreme case. Therefore, we determined that the cold water  
19 was being pumped from a maximum depth of 155 m and then intruded the coastal area. This  
20 finding reaches the maximum value that Narayan et al. (2010) proposed in which cooler waters  
21 from 100-150 m depths are able to be pumped via coastal upwelling.

22 To identify the movement path of cold water being pumped from the deep ocean, the starting  
23 time of SST drop was assessed at several stations in the research area, as shown in Figure 1.  
24 The analysis results of Typhoon Morakot ( $\Delta\text{SST} = 12.3^{\circ}\text{C}$ ) are shown in Table 4 as an example.  
25 The lag time shown in the table is the start time differences in the SST drops between the



1 stations for the Longdong buoy; in the table, a positive number indicates that the SST drop  
2 observed at the station occurred later than that observed at the Longdong buoy. As Table 4  
3 shows, we found that coastal SST drops occurred earliest in Longdong waters. We suggest,  
4 according to the bathymetry off northeast Taiwan, that the cold waters were pumped from the  
5 Kuroshio subsurface (~155 m depth) in the Okinawa Trough and reached the Longdong area  
6 first, and then, the cold water was transported north to Keelung and south to Suao, respectively.  
7 Figure 8 shows a sketch of the cold water movement path. This assumption can partially prove  
8 that no significant SST drop occurred at the Hualien buoy.

9 The exchange of water masses off northeastern Taiwan is complex. Chen et al. (1995) showed  
10 that at least six water masses take part in the mixing processes in this region, including the  
11 Kuroshio Surface Water (SW), Kuroshio Tropical Water (TW), Kuroshio Intermediate Water  
12 (IW), East China Sea Water (ECSW), Coastal Water (CW) and the Taiwan Strait Water (TSW).  
13 According to extensive investigations, the intrusion of the Kuroshio into the East China Sea  
14 (ECS) occurs northeast of Taiwan (Hsueh et al., 1992; Tang et al., 1999; Guo et al., 2006; Yang  
15 et al., 2011; Wu et al., 2017; Yang et al., 2018). The mechanism leading to the Kuroshio  
16 intrusion into the ECS is still being researched. Recently, Zhou et al. (2018) indicated that the  
17 Kuroshio subsurface water could intrude into the ECS shelf from northeast Taiwan and reach  
18 north of 29 degrees N. Yang et al. (2018) explained that a topographic beta spiral occurs when  
19 the Kuroshio encounters the shelf break and induces strong upwelling. These researchers  
20 suggested that the topographic beta spiral provides a dynamic channel to bring the cold deep  
21 water from Kuroshio to the continental shelf. Our findings in this study provide direct evidence  
22 from long-term buoy measurements.

### 23 **5.3 Spatial cold water intrusion**

24 In addition to coastal upwelling, the cold water in the coastal area of Longdong may also come  
25 from offshore surfaces, as many studies have confirmed that a cold dome exists in the waters



1 off northeastern Taiwan. Numerous observational and modeling studies have reported  
2 occurrences of cold water and isotherm doming in northeast Taiwan, which is known as the  
3 cold dome (Tang et al., 1999; Yang et al., 2011; Shen et al., 2011; Jan et al., 2011;  
4 Gopalakrishnan et al., 2013; Cheng et al., 2018). When the Kuroshio flows near the northeastern  
5 Taiwan shelf, a weaker northwestward branch intrudes the ECS shelf (Tang et al., 1999; Lee  
6 and Matsuno, 2007). Recently, Cheng et al. (2008) demonstrated a 4-6 year interannual  
7 variability in the cold dome. Then, the cold dome is formed because of the on-shelf intrusion  
8 of the Kuroshio subsurface water. Gopalakrishnan et al. (2013) established a numerical model  
9 and found that the cold dome occurrences appeared to be connected with the seasonal variability  
10 in the Kuroshio. Jan et al. (2011) used field observation data and satellite images to better  
11 understand that the center of the cold dome is located at approximately 25.625°N, 122.125°E.  
12 The diameter of the cold dome is approximately 100 km, and it has a weak counterclockwise  
13 circulation. The SST of the cold dome is ~ 3°C below the temperature of the ambient shelf  
14 waters.

15 Daily satellite images (Figure 9) show the spatial distribution of SSTs during Typhoon Jangmi  
16 in 2008. The cold dome moved shoreward along the movement of the typhoons. The  
17 temperature difference between the coastal area of Longdong and the center of the cold water  
18 is generally less than 3 °C. However, the scale of SST drop in the Longdong area was much  
19 higher. Although the contributions from the north (cold dome) and deep sea were not  
20 decomposed, it was suggested that cold water coming from the deep sea dominates the coastal  
21 SST drops in the Longdong area.

22

## 23 **6. Conclusions**

24 Seawater temperature affects marine environmental ecosystems and human activities. The  
25 variability in seawater temperature also influences typhoon intensity. It is widely known that



1 the SST may drop a few degrees after passage of a typhoon. However, in this study, we found  
2 that following summer typhoon passages in the coastal waters off Longdong in Taiwan, the SST  
3 may decrease to values lower than the annual minimum temperature (which always occurs in  
4 winter).

5 Long-term SST field data from the Longdong buoy (which is located 0.6 km offshore at a water  
6 depth of 23 m) over the past 20 years (1998 to 2017) were analyzed to study coastal SST drops.  
7 These decreases were observed after the passage of 43 typhoons. The mean SST drop during  
8 the 43 events was 6.1 °C. The lowest SST was 16.1 °C, which was observed during Typhoon  
9 Morakot in 2009; however, the maximum SST drop was 12.5 °C, observed during Typhoon  
10 Fungwong in 2008. This scale of decrease is much larger than that in the open ocean. The mean  
11 duration of the SST drop was 24 hours, and on average, 26.1 hours were required for the SST  
12 to recover to the background temperature.

13 Previous studies on the open ocean have proposed that the scale of SST drop is related to  
14 typhoon intensity and speed. However, we found that the scale of typhoon-induced coastal SST  
15 drops in the northeast Taiwan area were mainly correlated with the typhoon track. Typhoon  
16 intensity and moving speed do not appear to be significant factors driving coastal SST drops in  
17 this location. Typhoons that moved south of Longdong (i.e., Longdong is to the right side of the  
18 typhoon) accounted for more than 70% of coastal SST drops and exhibited extremely large  
19 decrease scales, irrespective of whether these typhoons traveled near or far from Longdong.

20 Wind-driven coastal upwelling was confirmed as the main mechanism involved in substantial  
21 coastal SST drops after typhoon passage at Longdong. The measurements indicated that many  
22 typhoons were accompanied by alongshore winds blowing in a constant direction. Such winds  
23 induce coastal upwelling and pump bottom seawater up to the surface. This was verified  
24 through measurements of the current profile collected at Longdong. This discovery explains the  
25 conclusion that SST drops are mainly influenced by typhoon tracks. However, the cold waters



1 were not directly supplied from the subsurface of Longdong. We suggest that the coldest water  
2 may originate from depths of 155 m in the Okinawa Trough, which is ~50 km from Longdong.  
3 These waters are the subsurface waters of Kuroshio. We found that the coverage of a large wind  
4 speed region by the Kuroshio is a significant factor that triggers the coastal SST drop. When  
5 the strong wind area largely overlapped with Kuroshio, there was a very large SST drop on the  
6 Longdong coast. By analyzing SST drop processes and the lag times between field stations, we  
7 suggest that the cold water intrudes first at Longdong and is then transported along the coast.  
8 Except for the vertical source of cold water, the cold waters from the known cold dome off  
9 northeastern Taiwan may also penetrate and cool the coastal area. An analysis of satellite images  
10 indicated that the cold dome moves towards the north coast of Taiwan after typhoon passage  
11 and contributes to coastal SST drops. In this study, the contributions of the offshore surface cold  
12 water and Kuroshio subsurface cold water were not decomposed, but we suggest that the  
13 Kuroshio subsurface cold water is the main source of the Longdong coastal SST drop. The  
14 presentation of the coastal SST dataset with significant drop may help to understand the  
15 interaction between Kuroshio with typhoons, and can be used to calibrate and validate the  
16 numerical models of such interactions.

17

18 **Author contributions.** D.J. Doong made the main contribution to this paper. He initiated the  
19 idea, collected the data, designed the experiment and wrote the manuscript. J.P. Peng worked  
20 on the data quality check, analysis and plotting the figures. A.V. Babanin joined the discussions  
21 and provided constructive suggestions on writing the manuscript.

22

23

24 **Competing interests.** The authors declare that they have no conflict of interest.

25

26

27 **Acknowledgements**



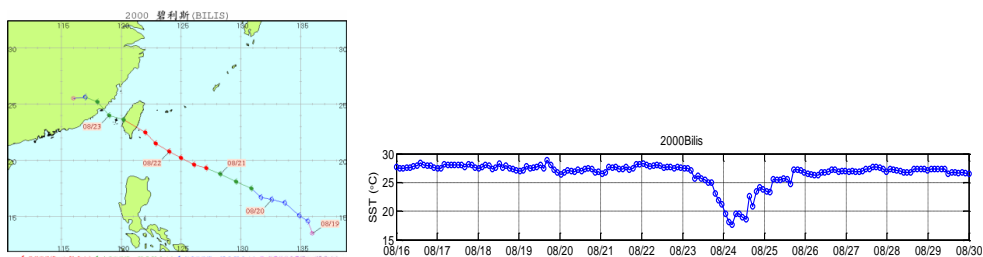
1 This research was performed with support from the Ministry of Science and Technology  
 2 (MOST) of Taiwan under grant no. MOST 106-2628-E-006-008-MY3. The buoys that measure  
 3 SST data are operated by the Coastal Ocean Monitoring Center of National Cheng Kung  
 4 University in Tainan, Taiwan. The authors would like to thank all their colleagues at the center.  
 5 In addition, the authors acknowledge the Industrial Technology Research Institute (ITRI) for  
 6 providing the ADCP current data.

7

8 **Appendix: Six cases of coastal SST drops larger greater than 10 °C observed by the**  
 9 **Longdong buoy after typhoon passage.** (Left figure shows the typhoon tracks,  
 10 and the time series of SSTs are shown on the right.)

11

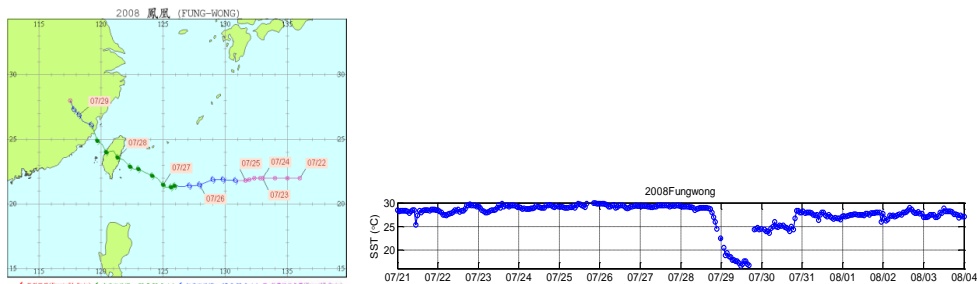
12 **(1) Typhoon Bilis in 2000, max.  $\Delta$ SST = 10.0 °C**



13

14

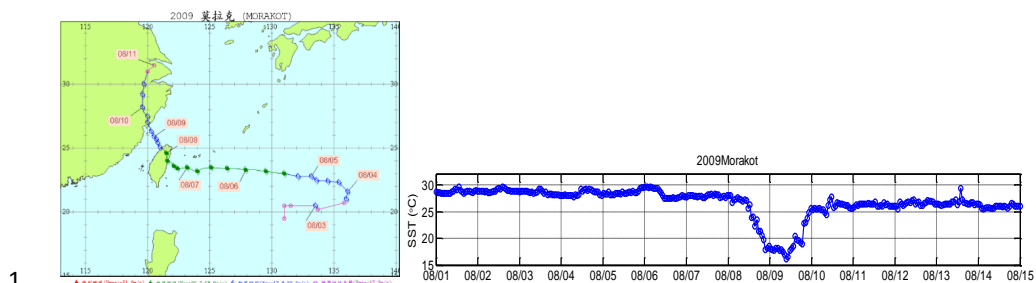
15 **(2) Typhoon Fungwong in 2008, max.  $\Delta$ SST = 12.5 °C**



16

17

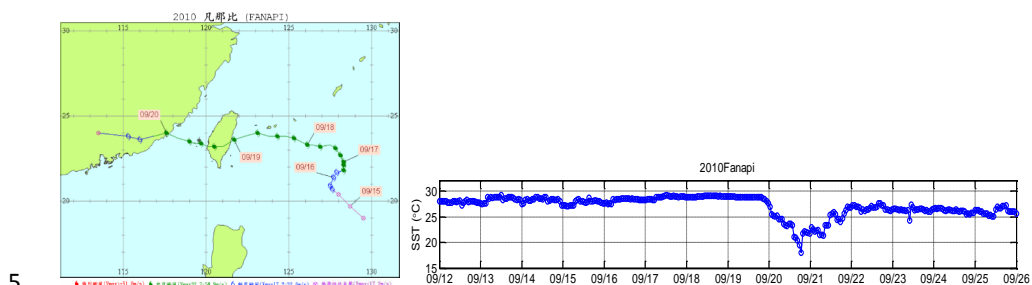
18 **(3) Typhoon Morakot in 2009, max.  $\Delta$ SST = 12.3 °C**



2

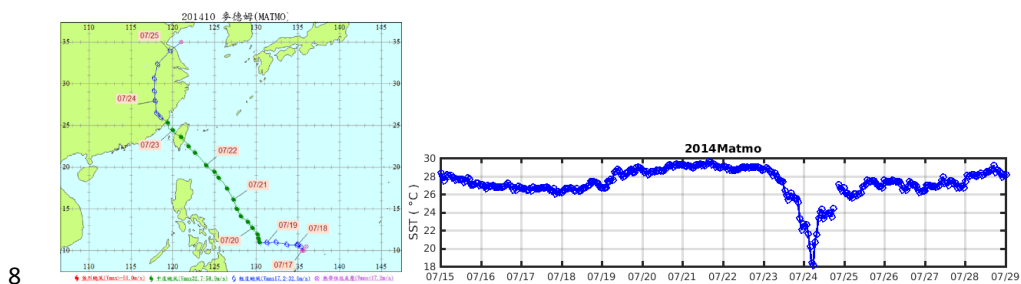
3

4 **(4) Typhoon Fanapi in 2010, max.  $\Delta$ SST = 10.5 °C**



6

7 **(5) Typhoon Matmo in 2014, max.  $\Delta$ SST = 10.4 °C**

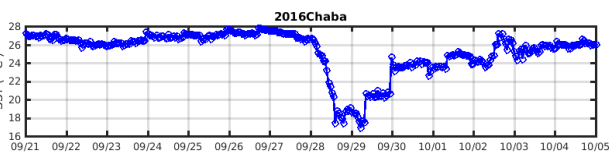
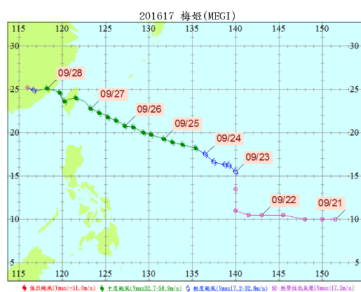


9

10 **(6) Typhoon Megi in 2016, max.  $\Delta$ SST = 10.0 °C**



1  
2





## 1 **References**

- 2 [1] Babin, S. M., Carton, J. A., Dickey, T. D., and Wiggert, J. D.: Satellite evidence of  
3 hurricane-induced phytoplankton blooms in an oceanic desert, *J. Geophys. Res.*, 109,  
4 C03043, <https://doi.org/10.1029/2003JC001938>, 2004.
- 5 [2] Bender, M. A., Ginis, I., and Kurihara, Y.: Numerical simulations of tropical cyclone-  
6 ocean interaction with a high-resolution coupled model, *J. Geophys. Res.*, 98, 23245-  
7 23263, <https://doi.org/10.1029/93JD02370> , 1993.
- 8 [3] Bingham, F. M.: Physical response of the coastal ocean to typhoon Isabel near landfall,  
9 *Ocean Sci.*, 3, 159-171, <https://doi.org/10.5194/os-3-159-2007>, 2007.
- 10 [4] Chang, Y., Liao, H. T., Lee, M. A., Chan, J. W., Shieh, W. J., Lee, K. T., Wang, G. H.,  
11 and Lan, Y. C.: Multisatellite observation on upwelling after the passage of typhoon Hai-  
12 Tang in the southern East China Sea, *Geophys. Res. Lett.*, 35, L03612,  
13 <https://doi.org/10.1029/2007GL032858>, 2008.
- 14 [5] Chen, C. T. A., Liu, C. T., Chuang, W. S., Yang, Y. J., Shiah, F. K., Tang, T. Y., and  
15 Chung, S. W.: Enhanced buoyancy and hence upwelling of subsurface Kuroshio waters  
16 after a typhoon in the southern East China Sea, *J. Marine Syst.*, 42, 65-79,  
17 [https://doi.org/10.1016/S0924-7963\(03\)00065-4](https://doi.org/10.1016/S0924-7963(03)00065-4), 2003.
- 18 [6] Chen, C. T. A., Ruo, R., Pai, S. C., Liu, C. T., and Wong, G. T. F.: Exchange of water  
19 masses between the East China Sea and the Kuroshio off northeastern Taiwan, *Cont.*  
20 *Shelf Res.*, 15, 19-39, [https://doi.org/10.1016/0278-4343\(93\)E0001-O](https://doi.org/10.1016/0278-4343(93)E0001-O), 1995.
- 21 [7] Chen, X., Pan, D., He, X., Bai, Y., and Wang, D.: Upper ocean responses to category 5  
22 typhoon Megi in the western north Pacific, *Acta Oceanol. Sin.*, 31, 51-58, 2012.



- 1 [8] Cheng, Y. H., Hu, J., Zheng, Q., and Su, F. C.: Interannual variability of cold domes  
2 northeast of Taiwan, *Int. J. Remote Sens.*, 39, 4293-4303,  
3 <https://doi.org/10.1080/01431161.2017.1395972>, 2018.
- 4 [9] Cheung, H. F., Pan, J., Gu, Y., and Wang, Z.: Remote sensing observation of ocean  
5 responses to typhoon Lupit in the northwest Pacific, *Int. J. Remote Sens.*, 34, 1478-1491,  
6 <https://doi.org/10.1080/01431161.2012.721940>, 2013.
- 7 [10] Chiang, T. L., Wu, C. R., and Oey, L. Y.: Typhoon Kai-Tak: an ocean's perfect storm, *J.*  
8 *Phys. Oceanogr.*, 41, 221-233, <https://doi.org/10.1175/2010JPO4518.1>, 2011.
- 9 [11] Chu, P. C., Veneziano, J. M., Fan, C., Carron, M. J., and Liu, W. T.: Response of the  
10 South China Sea to tropical cyclone Ernie 1996, *J. Geophys. Res.*, 105, 13991-14009,  
11 <https://doi.org/10.1029/2000JC900035>, 2000.
- 12 [12] Doong, D. J., Chen, S. H., Kao, C. C., and Lee, B. C.: Data quality check procedures of  
13 an operational coastal ocean monitoring network, *Ocean Eng.*, 34, 234-246,  
14 <https://doi.org/10.1016/j.oceaneng.2006.01.011>, 2007.
- 15 [13] Ghantous, M. and Babanin, A. V.: One-dimensional modelling of upper ocean mixing by  
16 turbulence due to wave orbital motion, *Nonlinear Proc. Geoph.*, 21, 325-338,  
17 <https://doi.org/10.5194/npg-21-325-2014>, 2014.
- 18 [14] Gopalakrishnan, G., Cornuelle, B. D., Gawarkiewicz, G., and McClean, J. L.: Structure  
19 and evolution of the cold dome off northeastern Taiwan: a numerical study,  
20 *Oceanography*, 26, 66-79, <https://doi.org/10.5670/oceanog.2013.06>, 2013.
- 21 [15] Gopalakrishna, V. V., Murty, V. S. N., Sarma, M. S. S., and Sastry, J. S.: Thermal  
22 response of upper layers of bay of Bengal to forcing of a severe cyclonic storm: a case  
23 study, *Indian J. Marine Sci.*, 22, 8-11, <http://drs.nio.org/drs/handle/2264/2897>, 1993.



- 1 [16] Guan, S., Zhao, W., Huthnance, J., Tian, J., and Wang, J.: Observed upper ocean  
2 response to typhoon Megi (2010) in the northern South China Sea. *J. Geophys. Res.-*  
3 *Oceans*, 119, 3134-3157, <https://doi.org/10.1002/2013JC009661>, 2014.
- 4 [17] Guo, X. Y., Miyazawa, Y., and Yamagata, T.: The Kuroshio onshore intrusion along the  
5 shelf break of the East China Sea: The origin of the Tsushima warm current, *J. Phys.*  
6 *Oceanogr.*, 36, 2205-2231, <https://doi.org/10.1175/JPO2976.1>, 2006.
- 7 [18] Hanshaw, M. N., Lozier, M. S., and Palter, J. B.: Integrated impact of tropical cyclones  
8 on sea surface chlorophyll in the North Atlantic, *Geophys. Res. Lett.*, 35, L01601,  
9 <https://doi.org/10.1029/2007GL031862>, 2008.
- 10 [19] Hsueh, Y., Wang, J., and Chern, C. S.: The intrusion of the Kuroshio across the  
11 continental shelf northeast of Taiwan, *J. Geophys. Res.*, 97, 14323-14330,  
12 <https://doi.org/10.1029/92JC01401>, 1992.
- 13 [20] Huang, C. J., Qiao, F., Dai, D., Ma, H., and Guo, J.: Field measurement of upper ocean  
14 turbulence dissipation associated with wave turbulence interaction in the South China  
15 Sea, *J. Geophys. Res.*, 117, C00J09, <https://doi.org/10.1029/2011JC007806>, 2012.
- 16 [21] Hung, C. C., Gong, G. C., Chou, W. C., Chung, C. C., Lee, M. A., Chen, H. Y., Huang,  
17 S. J., Yang, Y., Yang, W. R., Chung, W. C., Li, S. L., and Laws, E.: The effect of  
18 typhoon on particulate organic carbon flux in the southern East China Sea,  
19 *Biogeosciences*, 7, 3007-3018, <http://doi.org/10.5194/bgd-7-3521-2010>, 2010.
- 20 [22] Jan, S., Chen, C. C., Tsai, Y. L., Yang, Y. J., Wang, J., Chern, C. S., Gawarkiewicz, G.,  
21 Lien, R. C., Centurioni, L., and Kuo, J. Y.: Mean structure and variability of the cold  
22 dome northeast of Taiwan, *Oceanography*, 24, 100-109,  
23 <https://doi.org/10.5670/oceanog.2011.98>, 2011.



- 1 [23] Jan, S. and Chen, C. T. A.: Potential biogeochemical effects from vigorous internal tides  
2 generated in Luzon Strait: a case study at the southernmost coast of Taiwan, *J. Geophys.*  
3 *Res.- Oceans*, 1978-2012, <https://doi.org/10.1029/2008JC004887>, 2009.
- 4 [24] Jan, S., Wang, J., Yang, Y. J., Hung, C. C., Chern, C. S., Gawarkiewicz, G., Lien, R. C.,  
5 Centurion, L., Kuo, J. Y., and Wang, B.: Observation of a freshwater pulse induced by  
6 typhoon Morakot off the northern coast of Taiwan in August 2009, *J. Mar. Res.*, 71, 19-  
7 46, <https://doi.org/10.1357/002224013807343452>, 2013.
- 8 [25] Jiang, X. P., Zhong, Z., and Jiang, J.: Upper ocean response of the South China Sea to  
9 typhoon Krovanh (2003), *Dynam. Atmos. Oceans*, 47, 165-175,  
10 <https://doi.org/10.1016/j.dynatmoce.2008.09.005>, 2009.
- 11 [26] Kawai, Y. and Wada, A.: Detection of cyclone-induced rapid increases in chlorophyll-a  
12 with sea surface cooling in the northwestern Pacific Ocean from a MODIS/SeaWiFS  
13 merged satellite chlorophyll product, *Int. J. Remote Sens.*, 32, 9455-9471,  
14 <https://doi.org/10.1080/01431161.2011.562252>, 2011.
- 15 [27] Ko, D. S., Chao, S. Y., Wu, C. C., and Lin, I. I.: Impacts of typhoon Megi (2010) on the  
16 South China Sea, *J. Geophys. Res.-Oceans*, 119, 4474-4489,  
17 <https://doi.org/10.1002/2013JC009785>, 2014.
- 18 [28] Kuo, Y. C., Chern, C. S., Wang, J., and Tsai, Y. L.: Numerical study of upper ocean  
19 response to a typhoon moving zonally across the Luzon Strait, *Ocean Dynam.*, 61, 1783-  
20 1795, <http://doi.org/10.1007/s10236-011-0459-7>, 2011.
- 21 [29] Lee, J. S. and Matsuno, T.: Intrusion of Kuroshio water onto the continental shelf of the  
22 East China Sea, *J. Oceanogr.*, 63, 309-325, <http://doi.org/10.1007/s10872-007-0030-9>,  
23 2007.



- 1 [30] Lin, I. I., Liu, W. T., Wu, C. C., Chiang, J. C. H., and Sui, C. H.: Satellite observations  
2 of modulation of surface winds by typhoon-induced upper ocean cooling, *Geophys. Res.*  
3 *Lett.*, 30, 1131, <https://doi.org/10.1029/2002GL015674>, 2003.
- 4 [31] Lin, I. I., Liu, W. T., Wu, C. C., Wong, G. T. F., Hu, C., Chen, Z., Liang, W. D., Yang,  
5 Y., and Liu, K. K.: New evidence for enhanced ocean primary production triggered by  
6 tropical cyclone, *Geophys. Res. Lett.*, 30, 1718, <https://doi.org/10.1029/2003GL017141>,  
7 2003.
- 8 [32] Liu, X., Wang, M., and Shi, W.: A study of a hurricane Katrina-induced phytoplankton  
9 bloom using satellite observations and model simulations, *J. Geophys. Res.*, 114,  
10 C03023, <https://doi.org/10.1029/2008JC004934>, 2009.
- 11 [33] Liu, X. and Wei, J.: Understanding surface and subsurface temperature changes induced  
12 by tropical cyclones in the Kuroshio, *Ocean Dynam.*, 65, 1017–1027,  
13 <http://doi.org/10.1007/s10236-015-0851-9>, 2015.
- 14 [34] Matthews, J. B. R.: Comparing historical and modern methods of sea surface  
15 temperature measurement - part 1: review of methods, field comparisons and dataset  
16 adjustments, *Ocean Sci.*, 9, 683-694, <https://doi.org/10.5194/os-9-683-2013>, 2013.
- 17 [35] Morimoto, A., Kojima, S., Jan, S., and Takahashi, D.: Movement of the Kuroshio axis to  
18 the northeast shelf of Taiwan during typhoon events, *Estuar. Coast. Shelf S.*, 82, 547-  
19 552, <https://doi.org/10.1016/j.ecss.2009.02.022>, 2009.
- 20 [36] Narayan, N., Paul, A., Mulitza, S., and Schulz, M.: Trends in coastal upwelling intensity  
21 during the late 20th century, *Ocean Sci.*, 6, 815-823, [https://doi.org/10.5194/os-6-815-](https://doi.org/10.5194/os-6-815-2010)  
22 2010, 2010.



- 1 [37] Park, K. A, and Kim, K. R.: Unprecedented coastal upwelling in the East/Japan Sea and  
2 linkage to long-term large variations, *Geophys. Res. Lett.*, 37, L09603,  
3 <https://doi.org/10.1029/2009GL042231>, 2010.
- 4 [38] Price, J. F.: Upper ocean response to a typhoon, *J. Phys. Oceanogr.*, 11, 153-175,  
5 [https://doi.org/10.1175/1520-0485\(1981\)011<0153:UORTAH>2.0.CO;2](https://doi.org/10.1175/1520-0485(1981)011<0153:UORTAH>2.0.CO;2), 1981.
- 6 [39] Rao, A. D., Babu, S. V., and Dube, S. K.: Impact of a tropical cyclone on coastal  
7 upwelling processes, *Nat. Hazards*, 31, 415-435,  
8 <http://doi.org/10.1023/B:NHAZ.0000023360.37260.5b>, 2004.
- 9 [40] Sakaida, F., Kawamura, H., and Toba, Y.: Sea surface cooling caused by typhoons in the  
10 Tohoku area in August 1989, *J. Geophys. Res.*, 103, 1053-1065,  
11 <https://doi.org/10.1029/97JC01859>, 1998.
- 12 [41] Sanford, T. B., Price, J. F., and Girton, J. B.: Upper-ocean response to hurricane Frances  
13 (2004) observed by profiling EM-APEX floats, *J. Phys. Oceanogr.*, 41, 1041-1056,  
14 <https://doi.org/10.1175/2010JPO4313.1>, 2011.
- 15 [42] Shang, S. L., Li, L., Sun, F. Q., Wu, J. U., Hu, C. M., Chen, D. W., Ning, X. R. Qiu, U.,  
16 and Shang, S. P.: Changes of temperature and bio-optical properties in the South China  
17 Sea in response to typhoon Lingling, 2001, *Geophys. Res. Lett.*, 35, L10602,  
18 <https://doi.org/10.1029/2008GL033502>, 2008.
- 19 [43] Shen, M. L., Tseng, Y. H., and Jan, S.: The formation and dynamics of the cold-dome off  
20 northeastern Taiwan, *J. Marine Syst.*, 86, 10-27,  
21 <https://doi.org/10.1016/j.jmarsys.2011.01.002>, 2011.
- 22 [44] Siswanto, E., Ishizaka, J., Morimoto, A., Tanaka, K., Okumura, K., Kristijono, A., and  
23 Saino, T.: Ocean physics and biogeochemical responses to the passage of typhoon Maeri



- 1           in the East China Sea observed from Argo float and multiplatform satellites, *Geophys.*  
2           *Res. Lett.*, 35, L15604, <https://doi.org/10.1029/2008GL035040>, 2008.
- 3 [45] Siswanto, E., Ishizaka, J., Yokouchi, K., Tanaka, K., and Tan, C. K.: Estimation of  
4           interannual and interdecadal variations of typhoon-induced primary production: a case  
5           study for the outer shelf of the East China Sea, *Geophys. Res. Lett.*, 34, L03604,  
6           <https://doi.org/10.1029/2006GL028368>, 2007.
- 7 [46] Subrahmanyam, M. V.: Impact of typhoon on the north-west Pacific sea surface  
8           temperature: a case study of typhoon Kaemi (2006), *Nat. Hazards*, 78, 569-582,  
9           <https://doi.org/10.1007/s11069-015-1733-7>, 2015.
- 10 [47] Subrahmanyam, B., Rao, K. H., Rao, N. S., Murty, V. S. N., and Sharp, R. J.: Influence  
11           of a tropical cyclone on chlorophyll-a concentration in the Arabian Sea, *Geophys. Res.*  
12           *Lett.*, 29, 2065, <https://doi.org/10.1029/2002GL015892>, 2002.
- 13 [48] Sun, J., Oey, L. Y., Chang, R., Xu, F., and Huang, S. M.: Ocean response to typhoon  
14           Nuri (2008) in western Pacific and South China Sea, *Ocean Dynam.*, 65, 735-749,  
15           <http://doi.org/10.1007/s10236-015-0823-0>, 2015.
- 16 [49] Tang, T., Hsueh, Y., Yang, Y., and Ma, J.: Continental slope flow northeast of Taiwan, *J.*  
17           *Phys. Oceanogr.*, 29, 1353-1362, <https://doi.org/10.1175/1520->  
18           0485(1999)029<1353:CSFNOT>2.0.CO;2, 1999.
- 19 [50] Toffoli, A., McConochie, J., Ghantous, M., Loffredo, L., and Babanin, A. V.: The effect  
20           of turbulence induced by non-breaking waves on the ocean mixed layer: field  
21           observations on the Australian north-west shelf, *J. Geophys. Res.*, 117, C00J24,  
22           <https://doi.org/10.1029/2011JC007780>, 2012.



- 1 [51] Tsai, Y. L., Chern, C. S., and Wang, J.: Typhoon induce upper ocean cooling off  
2 northeastern Taiwan, *Geophys. Res. Lett.*, 35, L14605,  
3 <https://doi.org/10.1029/2008GL034368>, 2008a.
- 4 [52] Tsai, Y. L., Chern, C. S., and Wang, J.: The upper ocean response to a moving typhoon,  
5 *J. Oceanogr.*, 64, 115-130, <http://doi.org/10.1007/s10872-008-0009-1>, 2008b.
- 6 [53] Tsai, Y. L., Chern, C. S., Jan, S., and Wang, J.: Numerical study of cold dome variability  
7 induced by typhoon Morakot (2009) off northeastern Taiwan, *J. Mar. Res.*, 71, 109-132,  
8 <https://doi.org/10.1357/002224013807343434>, 2013.
- 9 [54] Tseng, Y. H., Jan, S., Dietrich, D. E., Lin, I. I., Chang, Y. T., and Tang, T. Y.: Modeled  
10 oceanic response and sea surface cooling to typhoon Kai-Tak, *Terr. Atmos. Ocean Sci.*,  
11 21, 85-98, <http://doi.org/10.3319/TAO.2009.06.08.02>, 2010.
- 12 [55] Wada, A.: Numerical simulations of sea surface cooling by a mixed layer model during  
13 the passage of typhoon Rex, *J. Oceanogr.*, 61, 41-57, [http://doi.org/10.1007/s10872-005-](http://doi.org/10.1007/s10872-005-0018-2)  
14 0018-2, 2005.
- 15 [56] Wada, A., Niino, H., and Nakano, H.: Roles of vertical turbulent mixing in the ocean  
16 response to typhoon Rex (1998), *J. Oceanogr.*, 65, 373-396,  
17 <http://doi.org/10.1007/s10872-009-0034-8>, 2009.
- 18 [57] Wei, J., Liu, X., and Wang, D. X.: Dynamic and thermal responses of the Kuroshio to  
19 typhoon Megi (2004), *Geophys. Res. Lett.*, 41, 8495–8502,  
20 <https://doi.org/10.1002/2014GL061706>, 2014.
- 21 [58] Wentz, F. J., Scott, J., Hoffman, R., Leidner, M., Atlas, R., and Ardizzone, J.: Remote  
22 sensing systems cross-calibrated multi-platform (CCMP) 6-hourly ocean vector wind  
23 analysis product on 0.25 deg grid, version 2.0, remote sensing system, Santa Rosa,



- 1 California. Available online at [www.remss.com/measurements/ccmp](http://www.remss.com/measurements/ccmp). [accessed in  
2 August 2018.], 2015.
- 3 [59] Wentz, F. J., Gentemann, C., Smith, D., and Chelton, D.: Satellite measurements of sea  
4 surface temperature through clouds. *Science*, 288, 847-850,  
5 <http://doi.org/10.1126/science.288.5467.847>, 2000.
- 6 [60] Wu, C. R., Chang, Y. L., Oey, L. Y., Chang, C. W. and Hsin, Y. C.: Air-sea interaction  
7 between tropical cyclone Nari and Kuroshio, *Geophys. Res. Lett.*, 35, L12605,  
8 <https://doi.org/10.1029/2008GL033942>, 2008.
- 9 [61] Wu, C. R., Wang, Y. L., Lin, Y. F., and Chao, S. Y.: Intrusion of the Kuroshio into the  
10 South and East China Seas, *Sci. Rep.*, 7, 7895, [http://doi.org/10.1038/s41598-017-08206-](http://doi.org/10.1038/s41598-017-08206-4)  
11 4, 2017.
- 12 [62] Xu, F., Yao, Y., Oey, L., and Lin, Y.: Impacts of pre-existing ocean cyclonic circulation  
13 on sea surface chlorophyll-a concentrations off northeastern Taiwan following episodic  
14 typhoon passages, *J. Geophys. Res.-Oceans*, 122, 6482-6497,  
15 <https://doi.org/10.1002/2016JC012625>, 2017.
- 16 [63] Yang, D. Z., Huang, R. X., Yin, B. S., Feng, X. R., Chen, H. Y., Qi, J. F., Xu, L. J., Shi,  
17 Y. L., Cui, X., Gao, G. D., and Benthuyssen, J. A.: Topographic beta spiral and onshore  
18 intrusion of the Kuroshio current, *Geophys. Res. Lett.*, 45, 287-296,  
19 <https://doi.org/10.1002/2017GL076614>, 2018.
- 20 [64] Yang, D. Z., Yin, B. S., Liu, Z. L., and Feng, X. R.: Numerical study of the ocean  
21 circulation on the East China Sea shelf and a Kuroshio bottom branch northeast of  
22 Taiwan in summer, *J. Geophys. Res.*, 116, C05015,  
23 <https://doi.org/10.1029/2010JC006777>, 2011.



- 1 [65] Zheng, Z. W., Ho, C. R., Zheng, Q., Lo, Y. T., Kuo, N. J., and Gopalakrishnan, G.:
- 2 Effects of preexisting cyclonic eddies on upper ocean responses to Category 5 typhoons
- 3 in the western North Pacific, *J. Geophys. Res.*, 115, C09013,
- 4 <https://doi.org/10.1029/2009JC005562>, 2010.
- 5 [66] Zheng, Z. W., Zheng, Q., Lee, C. Y., and Gopalakrishnan, G.: Transient modulation of
- 6 Kuroshio upper layer flow by directly impinging typhoon Morakot in east of Taiwan in
- 7 2009, *J. Geophys. Res.-Oceans*, 119, 4462-4473, <https://doi.org/10.1002/2014JC010090>,
- 8 2014.
- 9 [67] Zhou, P., Song, X. X., Yuan, Y. Q., Cao, X. H., Wang, W. T., Chi, L. B., and Yu, Z. M.:
- 10 Water mass analysis of the East China Sea and interannual variation of Kuroshio
- 11 subsurface water intrusion through an optimum multiparameter method, *J. Geophys.*
- 12 *Res.-Oceans*, 123, 3723-3738, <https://doi.org/10.1029/2018JC013882>, 2018.
- 13 [68] Zhu, T. and Zhang, D. L.: The impact of the storm-induced SST cooling on typhoon
- 14 intensity, *Adv. Atmos. Sci.*, 23, 14-22, <http://doi.org/10.1007/s00376-006-0002-9>, 2006.
- 15



1

2 **List of Table Captions:**

3 Table 1 Records of SST drops due to typhoon passage in the literature

4 Table 2 List of field SST data used in this study

5 Table 3 Significant SST drops observed at the Longdong buoy (N.E. Taiwan coast) during 43

6 typhoon passages from 1998 to 2017

7 Table 4 Quantities of SST drop, the lowest SST and their lag time corresponding to the

8 Longdong buoy during Typhoon Morakot in 2009. A positive lag time value indicates that the

9 SST drop observed at the station occurred later than that observed at the Longdong buoy. “-

10 “ means no significant SST drop observed.

11



1

Table 1 Records of SST drops due to typhoon passage in the literature

Sea area	SST drop	Typhoon	Main analysis data	Reference
Various Regions	1-8°C	16 typhoons from 1958 to 1988	Modeling	Bender et al. (1993)
Gulf of Mexico	2°C	Eloise in 1975	Field data	Price (1981)
N.W. Pacific (off Taiwan coast)	8°C	Gerald in 1987	Field data	Tsai et al (2008)
N.W. Pacific (off Japan coast)	9°C	T8914/T8915 in 1989	Satellite image	Sakaida et al. (1998)
SCS	1°C	Ernie in 1996	Modeling	Chu et al. (1996)
N.W. Pacific (off Taiwan coast)	9°C	Herb in 1996	R/V data	Chen et al (2003)
India Ocean	6-7°C	Chennai in 1997	Modeling	Rao et al (2004)
N.W. Pacific	3°C	Rex in 1998	Modeling & R/V data	Wada et al (2005; 2009)
N. SCS	9°C	Kaitak in 2000	Modeling	Tseng et al (2010)
N. SCS	10.8°C	Kaitak in 2000	Modeling	Chiang et al (2011)
M. SCS	11°C	Lingling in 2001	Satellite image	Shang et al (2008)
N.W. PO (off Taiwan coast)	5°C	Nari in 2001	Satellite image	Wu et al (2008)
N. SCS	5.3°C	Krovanh in 2003	Modeling	Jiang et al (2009)
N.W. Pacific (Luzon Strait)	1.8°C	Dujuan in 2003	Modeling	Kuo et al (2011)
N.E. Pacific (N. Carolina)	1-3°C	Isabel in 2003	Field data	Bingham (2007)
N.W. Pacific (Kuroshio region)	3°C	Megi in 2004	Satellite image	Wei et al. (2014)
N.W. Pacific (Kuroshio region)	4°C	Morakot in 2009	Modeling and Argo data	Zheng et al. (2014)
N.W. Pacific (off Taiwan coast)	4.5°C	Haitang in 2005	Satellite image	Chang et al (2008)
N.W. Pacific (off Taiwan coast)	13°C	Haitang in 2005	Field data	Morimoto et al (2009)
N.W. Pacific (Luzon Strait)	3.5°C	Pabuk in 2007	Modeling	Kuo et al (2011)
N.W. Pacific (off Taiwan coast)	2-4°C	Fungwong in 2008	R/V data	Hung et al (2010)
SCS	5-6°C	Nuri in 2008	Modeling	Sun et al. (2015)
N.W. Pacific	2°C	Kaemi in 2006	Satellite image	Subrahmanyam (2015)
N.W. Pacific	0.61-	22 typhoons from	SST maps and	Liu and Wei



(Kuroshio region)	4.93°C	2001 to 2010	Argo data	(2015)
N.W. Pacific (off Taiwan coast)	7°C	Morakot in 2009	Modeling	Tsai et al (2013)
SCS	8°C	Megi in 2010	Modeling & Satellite image	Ko et al. (2014)
SCS	4.2°C	Megi in 2010	Modeling & Mooring	Guan et al. (2014)

1

2



1

Table 2 List of field data used in this study

Data Type	Instrument Type	Station Name	Location	Depth (m)	Sampling interval (hour)	Accuracy (°C or m/s)
SST	Buoy	Longdong	121.9219 E; 25.0983 N	23	1 / 2*	0.1
SST	Buoy	Gueishandao	121.9233 E; 24.8469 N	38	1 / 2*	0.1
SST	Buoy	Suao	121.8800 E; 24.6194 N	20	1 / 2*	0.1
SST	Buoy	Hualien	121.6308 E; 24.0356 N	21	1	0.1
SST	Tide Station	Keelung	121.7442 E; 25.1572 N	5	1	0.1
SST	Tide Station	Fulong	121.9500 E; 25.0217 N	5	1	0.1
SST and Current	ADCP	Longdong	121.9219 E; 25.0983 N	23	1	0.1
SST	ADCP	Linshanbi	121.5103 E; 25.2839 N	24	0.1	0.1

2 \* All buoys have sampling interval 2 hours from 1998 to 2003 and 1 hour from 2004 to 2017.

3



Table 3 Significant SST drops observed at the Longdong buoy (N.E. Taiwan coast) during 43 typhoon passages from 1998 to 2017

No	Typhoon name	Typhoon dates	Track category*	Intensity category*	Moving speed* (m s <sup>-1</sup> )	Maximum sustained wind* (m/s)	Max. Hs (m)	ΔSST	Duration of SST drop (hr)	Duration of SST recovery (hr)	Cooling rate (°C/hr)
1	Zeb	1998/10/10-10/17	D	V	6.1	38	6.0	3.7	14	20	0.26
2	Babs	1998/10/14-10/30	E	IV	4.2	15	3.6	2.4	28	4	0.09
3	Maggie	1999/6/1-6/9	C	III	6.7	38	4.3	5.6	14	26	0.40
4	Kaitak	2000/7/3-7/12	D	I	10.6	30	2.4	3.5	46	50	0.08
5	Bilis	2000/8/18-8/27	B	V	6.1	53	5.0	10.0	12	24	0.83
6	Xangsane	2000/9/25-10/2	D	III	9.2	33	4.9	2.8	28	92	0.10
7	Chebi	2001/6/19-6/24	E	III	8.1	33	2.5	3.5	24	20	0.15
8	Utor	2001/7/1-7/7	C	I	9.2	38	5.1	9.0	24	12	0.38
9	Toraji	2001/7/25-8/1	B	III	4.7	38	3.2	3.6	18	12	0.20
10	Nari	2001/9/5-9/21	A	III	1.7	40	2.3	2.6	11	27	0.24
11	Lekima	2001/9/22-9/30	B	II	1.4	35	4.4	7.6	26	38	0.29
12	Morakot	2003/7/31-8/4	B	I	5.3	23	1.7	4.0	28	32	0.14
13	Dujuan	2003/8/27-9/3	C	IV	8.3	43	5.4	6.0	12	28	0.50
14	Mindulle	2004/6/21-7/4	D	IV	4.2	28	3.9	8.0	15	26	0.53
15	Nockten	2004/10/14-10/26	B	III	5.6	40	8.2	3.5	11	5	0.32
16	Matsa	2005/7/30-8/8	A	II	3.9	40	5.2	3.4	23	14	0.15
17	Sanvu	2005/8/9-8/14	C	I	6.4	20	3.2	7.3	23	6	0.32
18	Longwang	2005/9/25-10/3	B	IV	6.4	51	7.5	6.7	22	14	0.30
19	Chanchu	2006/5/8-5/18	E	IV	11.9	25	2.7	3.5	24	6	0.15
20	Bilis	2006/7/8-7/16	B	TS	5.0	25	4.8	5.3	12	30	0.44



21	Kaemi	2006/7/17-7/27	B	I	4.7	38	3.3	7.6	30	47	0.25
22	Sepat	2007/8/12-8/20	B	V	5.6	48	4.8	9.5	30	8	0.32
23	Kalmaegi	2008/7/13-7/20	B	II	5.6	33	3.1	5.1	15	18	0.34
24	Fungwong	2008/7/23-7/30	B	II	4.7	43	7.9	12.5	17	35	0.74
25	Sinlaku	2008/9/8-9/21	B	IV	2.2	38	7.3	6.8	18	20	0.38
26	Jangmi	2008/9/23-10/1	B	V	5.0	51	11.2	8.0	19	44	0.42
27	Morakot	2009/8/2-8/11	B	I	3.3	35	8.2	12.3	20	16	0.62
28	Merant	2010/9/6-9/10	C	I	3.3	15	1.5	4.6	26	42	0.18
29	Fanapi	2010/9/14-9/21	B	III	5.6	45	7.2	10.5	21	26	0.50
30	Nanmadol	2011/8/21-8/31	C	V	2.5	35	2.9	8.9	27	30	0.33
31	Saola	2012/7/26-8/5	B	II	4.2	30	8.3	5.4	10	14	0.54
32	Tembin	2012/8/17-8/30	D	IV	3.1	30	2.5	3.8	10	42	0.38
33	Trami	2013/8/16-8/24	A	I	12.8	30	3.1	2.4	21	10	0.11
34	Usagi	2013/9/16-9/24	C	V	5.3	53	4.3	6.4	20	41	0.32
35	Hagibis	2014/6/13-6/18	E	TS	3.6	15	1.0	4.5	76	60	0.06
36	Matmo	2014/7/16-7/25	B	II	5.6	38	4.3	10.4	22	29	0.47
37	Fungwong	2014/9/17-9/24	D	TS	6.1	25	3.4	3.5	43	10	0.08
38	Nepartak	2016/7/2-7/10	B	V	4.7	55	3.6	7.5	36	29	0.21
39	Meranti	2016/9/8-9/16	C	V	5.6	58	3.9	8.3	21	19	0.40
40	Megi	2016/9/22-9/29	B	IV	6.4	45	12.5	10.0	29	18	0.34
41	Aere	2016/10/4-10/14	C	TS	6.4	18	3.9	2.6	42	46	0.06
42	Nesat	2017/7/25-7/30	B	II	4.2	40	2.4	6.3	11	22	0.57
43	Hato	2017/8/19-8/24	C	III	7.8	20	2.0	5.0	51	9	0.10

1 \* indicates that the values were obtained when typhoons were close to Taiwan.



1

2 Table 4 Quantities of SST drop, the lowest SST and their lag time corresponding to  
 3 the Longdong buoy during Typhoon Morakot in 2009. A positive lag time value  
 4 indicates that the SST drop observed at the station occurred later than that observed at  
 5 the Longdong buoy. “-“ means no significant SST drop observed.

SST Station	Lowest SST (°C)	$\Delta$ SST (°C)	Lag time (hr)
Linshanbi	27.0	< 2°C	-
Keelung	24.7	2.6	+10
Longdong	16.1	12.3	0
Fulong	20.7	7.8	+1
Guishandao	19.9	8.1	+3
Suao	17.9	11.4	+6
Hualien		< 2°C	-

6

7



1 **List of Figure Captions:**

2 Figure 1 Locations of the study area and field stations. The gray belt is the main  
3 stream of Kuroshio; however, the dashed gray belt is the shift of Kuroshio during  
4 Typhoon Haitang in 2005 according to measurements by Morimoto et al. (2009)

5 Figure 2 SST drop observed by various types of instruments during Typhoon Usagi in  
6 2013

7 Figure 3 The significant SST drop event after the passage of Typhoon Fungwong in  
8 2008. (a) The typhoon track; (b) SST; (c) wind speed and direction; and (d)  
9 significant wave height. The data were observed by a data buoy in the Longdong  
10 coastal waters of northeast Taiwan.

11 Figure 4 Distribution of the SST drop magnitude for 43 typhoons

12 Figure 5 The SST drops for various typhoon tracks. The two numbers in parentheses  
13 show the typhoon number and the mean SST drop magnitude in the corresponding  
14 typhoon track.

15 Figure 6 Wind patterns at the time close to the start of the SST drop. (a) Typhoon Bilis  
16 in 2000. The SST started to decrease on 2000/8/23 at 10:00. The wind pattern was  
17 observed on 2000/8/23 at 08:00. (b) Typhoon Fungwong in 2008. The SST started to  
18 decrease on 2008/7/28 at 18:00. The wind pattern was observed on 2008/7/28 at  
19 20:00. (c) Typhoon Morakot in 2009. The SST started to decrease on 2009/8/8 at



1 13:00. The wind pattern was observed on 2009/8/8 at 14:00. (d) Typhoon Fanapi in  
2 2010. The SST started to decrease on 2010/9/19 at 22:00. The wind pattern was  
3 observed on 2010/9/19 at 20:00

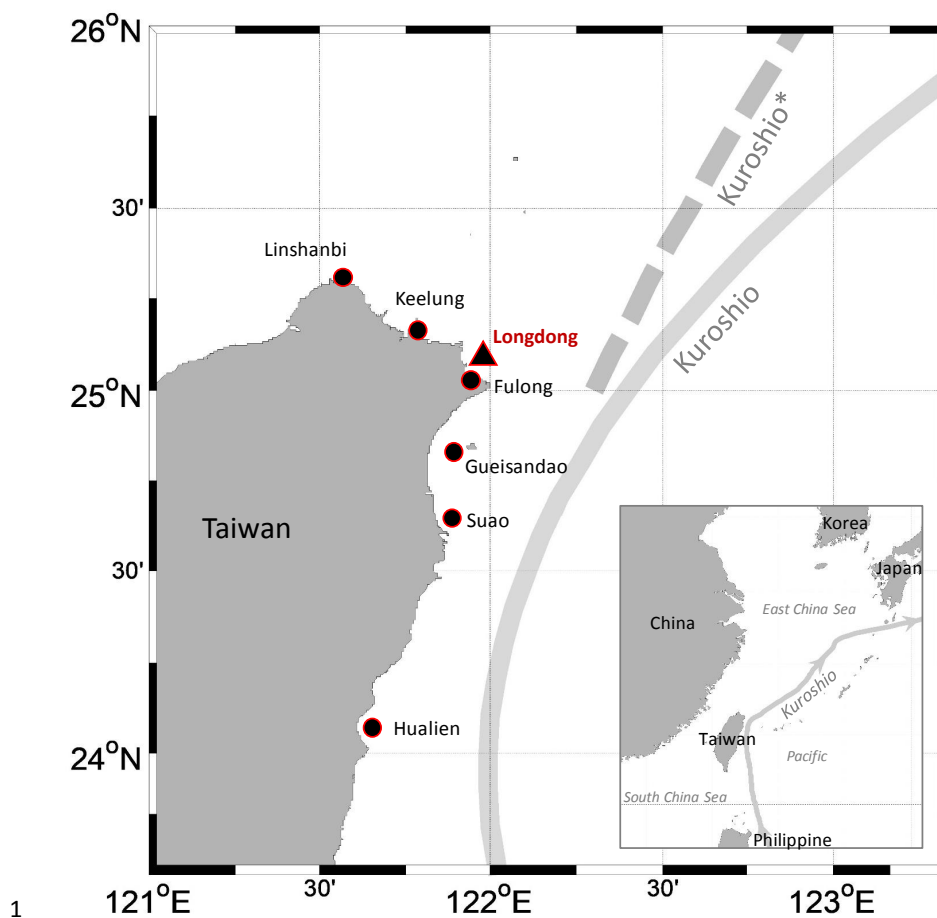
4 Figure 7 Current profile and corresponding tide level observed in Longdong during  
5 Typhoon Fungwong in 2008

6 Figure 8 The suggested movement path of cold water. The cold water was pumped  
7 from the Kuroshio subsurface in the Okinawa Trough and reached the Longdong  
8 coastal waters first. Then, the cold water was transported north to Keelung and south  
9 to Suao.

10 Figure 9 Movement of the cold dome off northeast Taiwan during Typhoon Jangmi in  
11 2008. The typhoon track is shown in the upper panel. The lower panel shows the  
12 satellite images of SST.

13

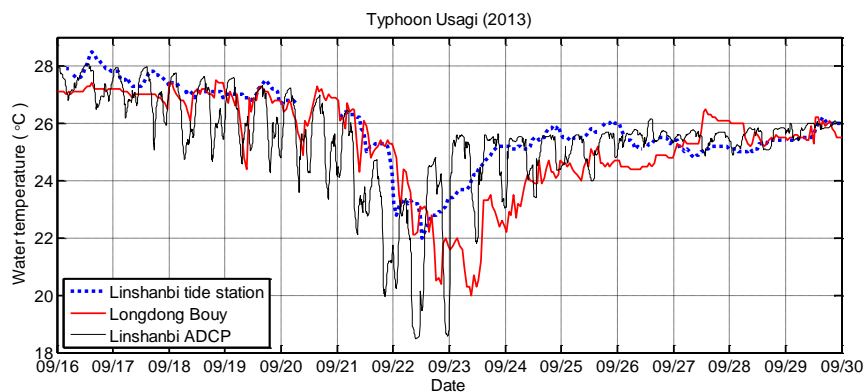
14



1

2 Figure 1 Locations of the study area and field stations. The gray belt is the main  
3 stream of Kuroshio; however, the dashed gray belt is the shift of Kuroshio during  
4 Typhoon Haitang in 2005 according to measurements by Morimoto et al. (2009)

5



1

2 Figure 2 SST drop observed by various types of instruments during Typhoon Usagi in

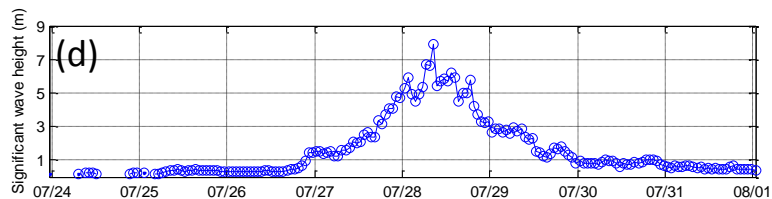
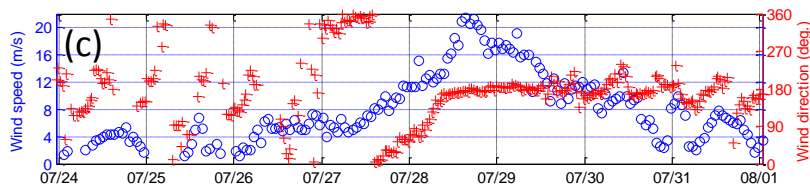
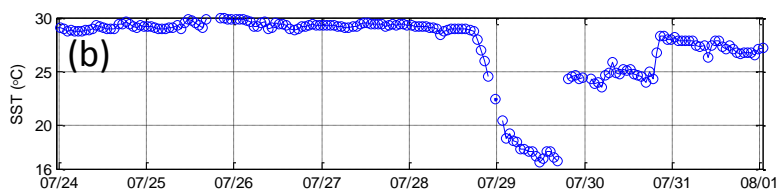
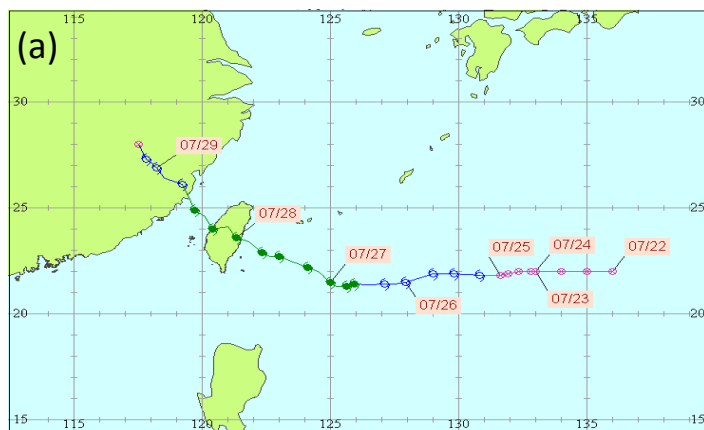
3

2013

4



1



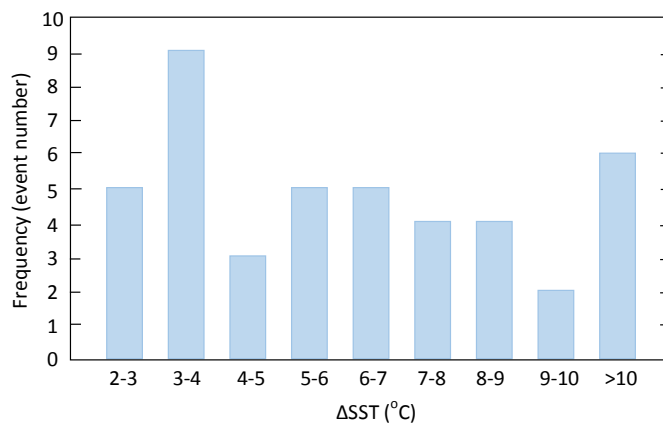
2

3 Figure 3 The significant SST drop event after the passage of Typhoon Fungwong in

4 2008. (a) The typhoon track; (b) SST; (c) wind speed and direction; and (d)

5 significant wave height. The data were observed by a data buoy in the Longdong

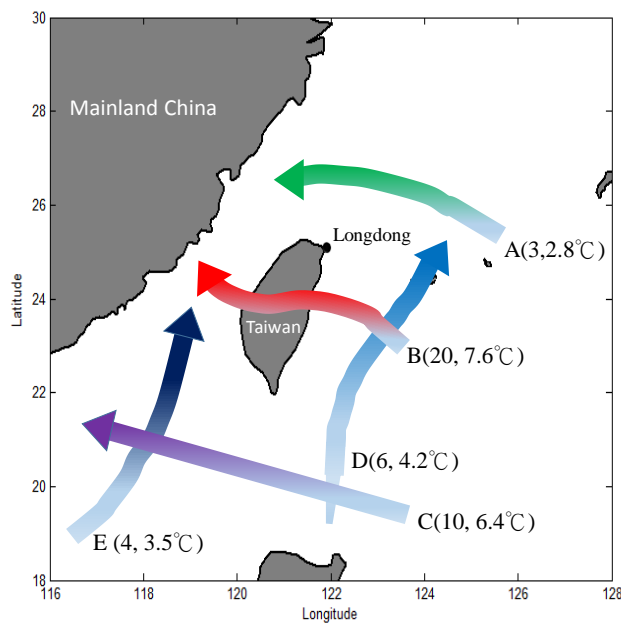
6 coastal waters of northeast Taiwan.



1

2

Figure 4 Distribution of the SST drop magnitude for 43 typhoons

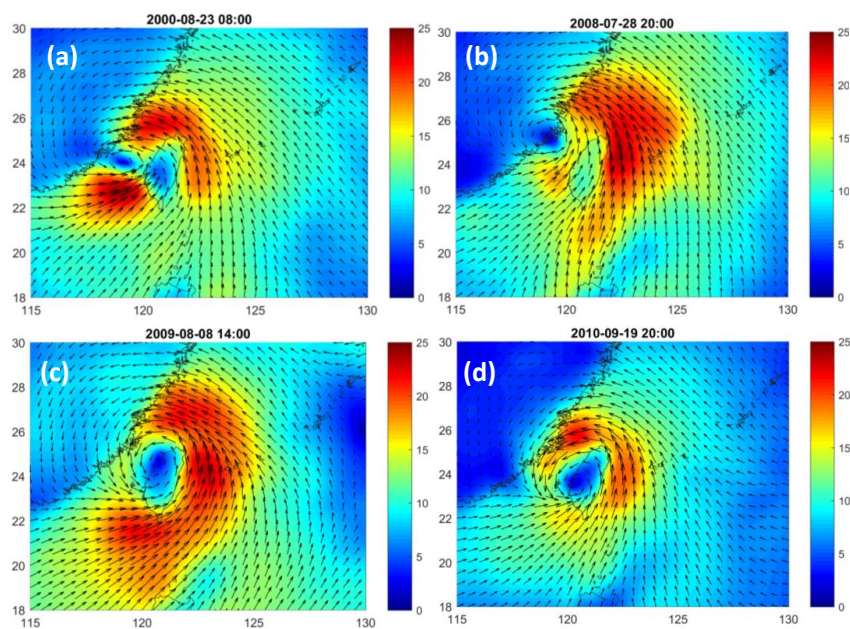


3

4 Figure 5 The SST drops for various typhoon tracks. The two numbers in parentheses

5 show the typhoon number and the mean SST drop magnitude in the corresponding

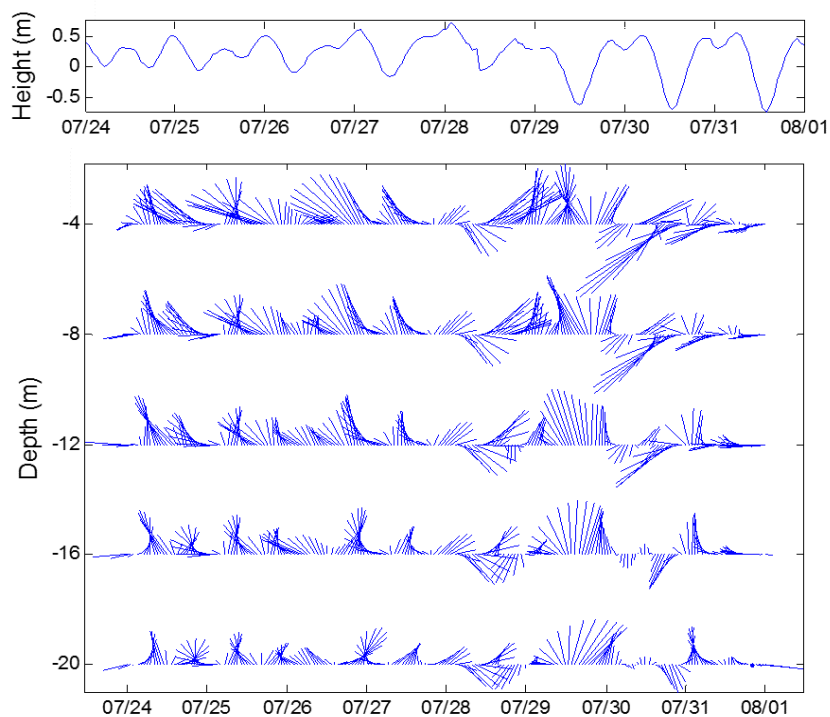
6 typhoon track.



1

2 Figure 6 Wind patterns at the time close to the start of the SST drop. (a) Typhoon Bilis  
 3 in 2000. The SST started to decrease on 2000/8/23 at 10:00. The wind pattern was  
 4 observed on 2000/8/23 at 08:00. (b) Typhoon Fungwong in 2008. The SST started to  
 5 decrease on 2008/7/28 at 18:00. The wind pattern was observed on 2008/7/28 at 20:00.  
 6 (c) Typhoon Morakot in 2009. The SST started to decrease on 2009/8/8 at 13:00. The  
 7 wind pattern was observed on 2009/8/8 at 14:00. (d) Typhoon Fanapi in 2010. The SST  
 8 started to decrease on 2010/9/19 at 22:00. The wind pattern was observed on 2010/9/19  
 9 at 20:00

10



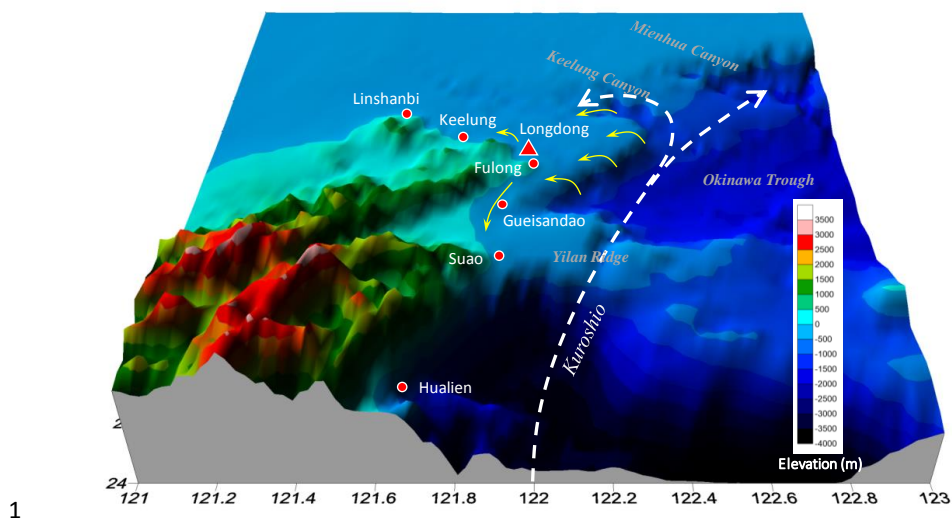
1

2 Figure 7 Current profile and corresponding tide level observed in Longdong during

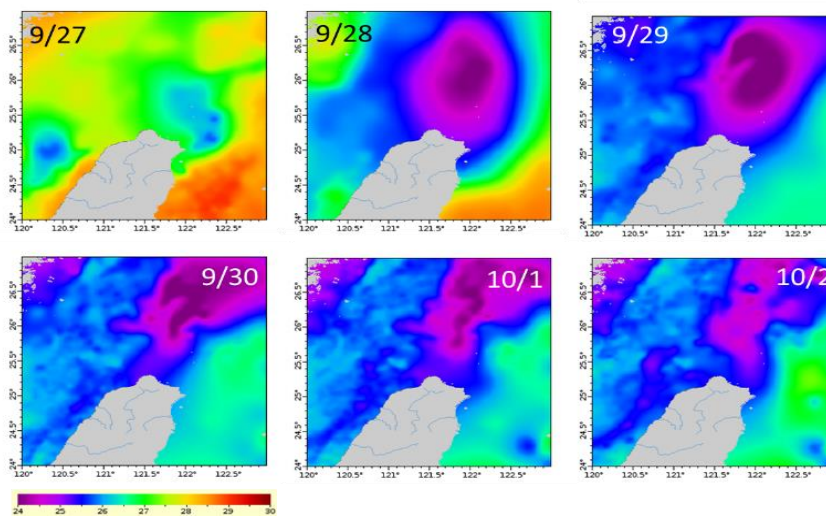
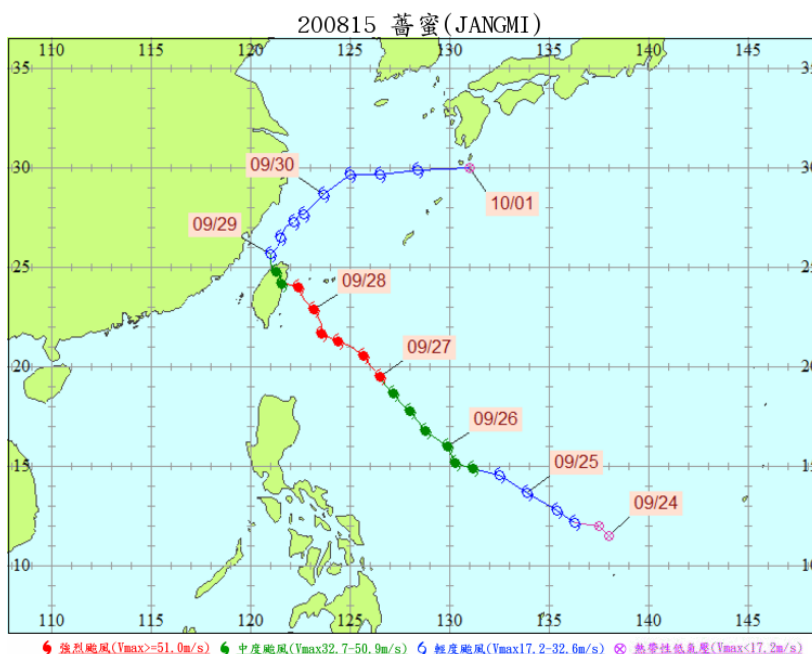
3

Typhoon Fungwong in 2008

4



1  
2 Figure 8 The suggested movement path of cold water. The cold water was pumped  
3 from the Kuroshio subsurface in the Okinawa Trough and reached the Longdong  
4 coastal waters first. Then, the cold water was transported north to Keelung and south  
5 to Suao.



3 Figure 9 Movement of the cold dome off northeast Taiwan during Typhoon Jangmi in  
 4 2008. The typhoon track is shown in the upper panel. The lower panel shows the  
 5 satellite images of SST.